Improved Maneuver Reconstructions for the GRAIL Orbiters

Mason Keck*
NASA Space Grant Program
Mentor: Tung-Han You†
Co-Mentor: Peter Antreasian‡

September 20, 2012

Abstract

Maneuver reconstructions for the Gravity Recovery and Interior Laboratory (GRAIL) A and B lunar orbiters were improved through updates to the orbit determination filter and dynamic models. Consistent reconstructions of the 27 GRAIL A and B maneuvers from the Trans-Lunar Cruise phase in the fall of 2011 through the Transition to Science Formation phase in February 2012 were performed. Standard methods of orbit determination were applied incorporating the latest dynamic models and filter strategies developed by the GRAIL Navigation and Science Teams, including a high resolution, 420x420 degree and order lunar spherical harmonic gravity field model. For Trans-Lunar Cruise for GRAIL-A (TLC-A), all maneuvers executed with ΔV errors below 5.50 $\pm$0.50 mm/s and pointing errors below 0.25 degrees. GRAIL-A lunar orbit maneuvers had ΔV errors below 30.0 mm/s and pointing errors below 0.51 degrees. For TLC-B, all maneuvers executed with ΔV errors below 8.60 $\pm$1.41 mm/s and pointing errors below 0.300 degrees. GRAIL-B maneuvers in lunar orbit executed with maximum ΔV errors of 25.0 mm/s and pointing error of 0.43 degrees. These maneuver reconstructions will enable the GRAIL Navigation Team to better characterize the main engine performance of each spacecraft. This will help the Navigation Team to navigate low ($>$ 8 km) altitude orbits during the extended-mission phase in the fall of 2012.

1 Introduction

The Gravity Recovery and Interior Laboratory (GRAIL) science mission to map the Moon's gravity field will begin its extended mission phase at the end of August. GRAIL features two spacecraft, GRAIL-A and GRAIL-B, that accurately measure the spacecraft separation distance. From these measurements, the GRAIL Science Team has produced high-resolution lunar gravity fields with uncertainties that are 2 and 3 orders of magnitude lower for the near and far side of the Moon, respectively, than the previous best lunar gravity model, the Lunar Prospector LP150Q model, which was used in GRAIL navigation up to the end of the science phase. For the extended mission phase, The GRAIL navigation team has designed GRAIL orbits that come within 8 km of the lunar surface. Navigating these low-altitude orbits will require accurate models of all dynamic and

*Boston University Graduate Student, NASA Space Grant Summer Internship at Jet Propulsion Laborator, California Institute of Technology, 4800 Oak Grove Drive, Pasadenai, CA 91109-8099

†Inner-Planet Navigation Group Supervisor, Section 343A, Jet Propulsion Laborator, California Institute of Technology, 4800 Oak Grove Drive, Pasadenai, CA 91109-8099

‡GRAIL Navigation Team Chief, Section 343A, Jet Propulsion Laborator, California Institute of Technology, 4800 Oak Grove Drive, Pasadenai, CA 91109-8099

non-dynamic forces on the orbiters and the orbiter tracking data, including lunar gravity, main engine thrust, and atmospheric delay, used to analyze GRAIL orbiter tracking data. This report presents reconstructions of the 27 GRAIL orbiter maneuvers during the GRAIL-A and GRAIL-B Trans-Lunar Cruise (TLC), Lunar Orbit Insertion (LOI), Orbit Period Reduction (OPR), and Transition to Science Formation (TSF) phases using the most current dynamic and non-dynamic models and a consistent filter strategy.

2 Background: Orbit Determination

Orbit determination is the process of estimating a spacecraft's position and velocity, or state, in order to model and predict the spacecraft's trajectory. A spacecraft state is determined through minimizing the difference, or residuals, between the observable tracking data, O, and the computed model of a satellite's orbit, C.the Deep Space Network (DSN) receives S-band (2.10 GHz) data, which give line-of-sight Doppler shift and range data for a satellite [1]. To best estimate the spacecraft orbit, all forces on the spacecraft and influences on the tracking data are modeled. The spacecraft ephemeris is determined through numerically integrating the equations of motion describing the dynamic forces on the satellite. In order of decreasing magnitude, significant dynamic forces acting on the GRAIL spacecraft include lunar point-mass and oblate gravity, Earth point-mass gravity, solar pressure, relativistic effects, solar point-mass gravity, the lunar albedo, and the oblate gravity of the Earth. Dynamic forces also include angular momentum desaturation events, which are the firing of attitude control system (ACS) thrusters to relieve the net build-up of angular momentum on the spacecraft from solar pressure. Significant observational models include models of the troposphere, ionosphere, motion of the continental plates, DSN station locations, and signal travel time on circuitry on the spacecraft and the DSN networks.

A data analysis filter specifying a priori, or initial, uncertainties in parameter values guides the orbit determination analysis. Initial best estimates of the dynamic forces, non-dynamic forces, and filter make up the nominal trajectory solution. The residuals of the computed data and the observable data are minimized using least-square methods and statistical batch filters [3]. A good nominal solution allows for orbit determination to involve minimizing the residuals with linear, least-squares methods, i.e. solving for $\vec{x}$ in $\hat{A}\vec{x} = \vec{b}$, which involve minimizing the sum-of-squares of the difference $O - C$.

3 Methods

Orbit determination is carried out at JPL using the MONTE navigation software developed at JPL. MONTE has a database of models describing spacecraft dynamics,forces on a spacecraft, and non-dynamic observation influences. Common reference frames used in GRAIL orbit determination analysis include the Earth-Mean Equator and Equinox of J2000.0 coordinate frame (EME2000) and the Libration Moon Pole frame [1].

Analysis strategies included analyzing data over long data 'arcs' and using the most accurate dynamic force models available, particularly the highest resolution (420x420) lunar gravity field and reconstructed spacecraft attitude information. The filter strategy used was consistent for each science phase. Checks were made to ensure the correct dynamic, non-dynamic, and filter inputs were used in the analysis. The Epoch state and DCO were typically set to coincide with apoapsis. GRAIL TLC and LOI maneuver filter strategy involved estimations of the constant thrust force terms and maneuver burn duration. OPR maneuver filter strategy involved estimations of the constant and linear thrust force terms and burn duration. Final results were converted to total

change in velocity, ΔV, and pointing direction in terms of the spacecraft Y and Z coordinates. Stochastic models account for non-modeled forces. Maneuver burn duration was taken from ACS quick-look reports whenever possible and from ACS accelerometer telemetry data whenever quick-look reports were not available. Burn durations estimated from telemetry data agreed with the values from ACS quick-look reports to within 0.2 seconds for all cases. The epoch state typically was determined from a delivered orbit determination analysis during operations.

Each OPR and TSF maneuver was modeled with a 6th-order polynomial thrust model and a linear force model estimated from telemetry accelerometer data. Epoch states were taken from a reconstruction from GRAIL operations except for some OPR maneuvers were work when less than one orbit of data was included in any delivered orbit determination analysis. The data cutoff time (DCO) was determined to balance the inclusion of the data and the integrity of the fit. A 'DCO-stepping' strategy of fitting data before the maneuver and then allowing in more data after the maneuver was used frequently.

Filter inputs, including a priori, or initial, estimated uncertainties in parameters, and estimated parameters, were setup to estimate the constant thrust term of the maneuver model, which is modeled as a 6th order polynomial. In OPR analysis, the constant and linear thrust terms were estimated. Additionally, maneuver pointing angle with respect to the EME2000 RA and declination directions and duration are estimated in the filter. F_0 estimates were converted to ΔV estimates in the final analysis in order to compare the reconstructed solution and the reconstructed OD solution during operations.

Non-dynamic models of the ionosphere and troposphere are included but are not estimated in the filter process. 1-way and 3-way Doppler tracking data was ignored. Datum received with an elevation below 10 degrees was also ignored as atmospheric influence on radio signals is not modeled for low elevation angles.

After integration, obvious erroneous data and other non-physical data are removed from the fit. The data is then filtered and data weights are applied, which assumes that the amplitude of the residuals for a given pass are due to white noise. Data editing and filtering is carried out until the post-fit residuals have a near random profile. A fit is deemed acceptable if the total change in any given estimated parameter, Δq, is less than the parameter's a priori sigma, σq. If this is not true, then filter covariances and/or the dynamic model are updated, and filtering is redone and/or fitting process is restarted. If the fit is acceptable,the post-fit parameter values are used as the nominal values for a new integration of the equations of motion. This process is repeated until the model has converged to the data, which is indicated by a small difference between the pre-fit and post-fit residuals of the computed model and the data. The nominal OD process used in this analysis is summarized in Figure 1.

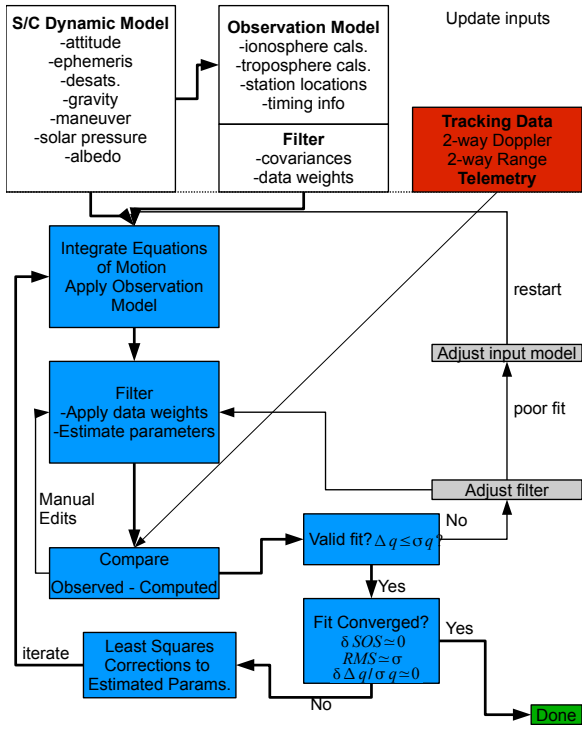

Figure 1: Orbit determination process in GRAIL maneuver reconstructions. Δq indicates the total change in a parameter value during a fit. σq indicates the a priori uncertainty of a parameter.

4 Results

Maneuver errors are reported in terms of ΔV error and pointing error in terms of spacecraft X and Y coordinates. The constant force term, F_0 and burn duration, was estimated, and F_0 error was converted to ΔV error in order to make comparisons with orbit determination (OD) analysis during operations. Maneuvers were found to have executed within 2 σ for pointing and 1 σ for ΔV for all maneuvers. For TLC-A, maximum ΔV error of 5.32 mm/s $\pm$0.37 mm/s, RA error of 0.2760 $\pm$ 0.008 degrees, and declination error of 0.1290 $\pm$ 0.0930 degrees were calculated. LOI-A executed with 0.07 degrees pointing error and 0.60 N F_0 error. For OPR-A, maximum GRAIL-A ΔV errors of -29.18 $\pm$0.70 mm/s, RA errors of -0.848 $\pm$ 0.0610 degrees and declination errors of 0.4030 $\pm$ 0.0120 degrees were calculated. For TSF-A, maximum ΔV errors of -3.85 $\pm$ 0.08 mm/s, RA errors of 0.3730 $\pm$ 0.0020 degrees, and declination error of 0.2680 $\pm$ 0.0008 degrees were calculated. Pointing error is consistently seen to be biased in the first quadrant in spacecraft coordinates for the OPR-A maneuvers.

For TLC-B, maximum ΔV error of -8.60 mm/s $\pm$1.41 mm/s, Maximum RA error of -0.2280 $\pm$ 0.0014 degrees and declination error of -0.3000 $\pm$ 0.0011 degrees were calculated. LOI-A executed with 0.30 degrees pointing error and 0.25 N error in the constant term, F_0, of the thruster force model. For OPR-B, maximum ΔV errors of -24.43 $\pm$0.74 mm/s, RA errors of -0.855 $\pm$ 0.0076 degrees, and declination errors of -0.1190 $\pm$ 0.0046 degrees were calculated. For TSF-B, maximum ΔV errors of -6.27 $\pm$ 0.21 mm/s, RA errors of -0.6250 $\pm$ 0.0025 degrees, and declination error of -0.083 ± 0.0008 degrees were calculated. Pointing error is also consistently biased in the first quadrant in spacecraft coordinates for the OPR-B maneuvers.

TLC maneuvers generally executed in pointing and ΔV within 3σ of the designed burn while several OPR maneuvers executed outside of 3σ error for pointing. Results and specific methods are discussed for each analyzed maneuver. A summary of GRAIL-A and GRAIL-B execution errors are given in Tables 1 and 2, respectively.

Maneuver	**RA (degrees)**	**DEC (degrees)**	**ΔV (mm/s)**	
Solution	**RA error (degrees)**	**Dec. error (degrees)**	**ΔV error (mm/s)**	Est. parameters
TCM-A2	0.0000 ± 0.1662	0.0000 ± 0.1662	13968.00 ± 11.87	
solution	0.2472 ± 0.0011	0.0050 ± 0.0032	0.34 ± 0.59	RA, DEC, F[0], Δt
TCM-A3	0.0000 ± 0.0859	0.0000 ± 0.0859	6454.00 ± 5.86	
solution	0.0246 ± 0.0016	0.0654 ± 0.0074	-2.62 ± 0.52	RA, DEC, F[0], Δt
TCM-A4	0.0000 ± 0.1318	0.0000 ± 0.1318	234.00 ± 1.34	
solution	0.0907 ± 0.0630	0.0963 ± 0.0974	-5.32 ± 0.37	RA, DEC, F[0], Δt
LOI-A*	0.0000 ± 0.2300	0.0000 ± 0.0830	33.5089 ± 0.6560	
solution	-0.3730 ± 0.0110	-0.4000 ± 0.0120	0.6034 ± 0.0008	RA, DEC, F[0], Δt
PRM-A1	0.0000 ± 0.1662	0.0000 ± 0.1662	79286.00 ± 66.11	
solution	0.3171 ± 0.0069	0.1869 ± 0.0046	-29.18 ± 0.70	RA, DEC, F[0], Δt
PRM-A2	0.0000 ± 0.1662	0.0000 ± 0.1662	79286.00 ± 66.11	
solution	0.2864 ± 0.0037	0.1894 ± 0.0092	-23.51 ± 0.40	RA, DEC, F[0], Δt
PRM-A3	0.0000 ± 0.1662	0.0000 ± 0.1662	79286.00 ± 66.11	
solution	0.1118 ± 0.0056	0.4911 ± 0.0241	-20.00 ± 0.97	RA, DEC, F[0], F[1], Δt
PRM-A4	0.0000 ± 0.1662	0.0000 ± 0.1662	69544.00 ± 58.00	
solution	0.1717 ± 0.0057	0.1851 ± 0.0315	-7.13 ± 0.34	RA, DEC, F[0], F[1], Δt
PRM-A5	0.0000 ± 0.1662	0.0000 ± 0.1662	69544.00 ± 58.00	
solution	0.1788 ± 0.0019	0.1593 ± 0.0045	-6.65 ± 0.32	RA, DEC, F[0], Δt
PRM-A6	0.0000 ± 0.1662	0.0000 ± 0.1662	69544.00 ± 58.00	
solution	0.2557 ± 0.0035	0.0618 ± 0.0053	-11.53 ± 0.36	RA, DEC, F[0], F[1], Δt
PRM-A7	0.0000 ± 0.1662	0.0000 ± 0.1662	69544.00 ± 58.00	
solution	0.2501 ± 0.0032	0.1174 ± 0.0033	18.62 ± 3.23	RA, DEC, F[0], Δt
TSM-A1	0.0000 ± 0.0859	0.0000 ± 0.0859	8234.00 ± 7.25	
solution	0.3274 ± 0.0006	-0.3146 ± 0.0020	-3.85 ± 0.08	RA, DEC, F[0], F[1], Δt
TSM-A2	0.0000 ± 0.0859	0.0000 ± 0.0859	19276.00 ± 16.23	
solution	0.0135 ± 0.0003	-0.0568 ± 0.0014	1.96 ± 0.21	RA, DEC, F[0], F[1], Δt

Table 1: Maneuver execution errors for the GRAIL-A spacecraft. Total pointing error is less than RA error in some cases as RA and declination are correlated. *LOI-A lists F_0 in Newtons for the thrust model instead of ΔV as the ΔV conversion was not available for LOI.

Maneuver	RA (degrees)	DEC (degrees)	ΔV (mm/s)	
Solution	**RA error (degrees)**	**Dec. error (degrees)**	**ΔV error (mm/s)**	Est. parameters
TCM-B2	0.0000 ± 0.1662	0.0000 ± 0.1662	25096.00 ± 21.04	
solution	-0.0539 ± 0.0007	0.3002 ± 0.0011	-8.60 ± 1.41	RA, DEC, F[0], Δt
TCM-B3	0.0000 ± 0.1662	0.0000 ± 0.1662	8845.00 ± 7.73	
solution	0.2181 ± 0.0014	0.1349 ± 0.0044	-2.54 ± 0.48	RA, DEC, F[0], F[1], Δt
TCM-B4	0.0000 ± 0.1261	0.0000 ± 0.1261	257.00 ± 1.47	
solution	-0.0108 ± 0.0688	-0.0249 ± 0.0573	-0.19 ± 0.36	RA, DEC, F[0], F[1], Δt
LOI-B*	0.0000 ± 0.2300	0.0000 ± 0.0830	34.1695 ± 0.2187	
solution	-0.3730 ± 0.0110	-0.4000 ± 0.0120	0.2510 ± 0.0008	RA, DEC, F[0], Δt
PRM-B1	0.0000 ± 0.0859	0.0000 ± 0.0859	74109.00 ± 61.80	
solution	0.1010 ± 0.0038	0.0714 ± 0.0031	13.98 ± 0.61	RA, DEC, F[0], F[1], Δt
PRM-B2	0.0000 ± 0.0859	0.0000 ± 0.0859	74109.00 ± 61.80	
solution	0.0650 ± 0.0006	0.0659 ± 0.0002	3.64 ± 0.63	RA, DEC, F[0], F[1], Δt
PRM-B3	0.0000 ± 0.0859	0.0000 ± 0.0859	74109.00 ± 61.80	
solution	0.0037 ± 0.0009	0.0545 ± 0.0002	-5.48 ± 0.61	RA, DEC, F[0], F[1], Δt
PRM-B4	0.0000 ± 0.0859	0.0000 ± 0.0859	70634.00 ± 58.91	
solution	0.0857 ± 0.0031	0.0822 ± 0.0053	18.21 ± 0.68	RA, DEC, F[0], F[1], Δt
PRM-B5	0.0000 ± 0.0859	0.0000 ± 0.0859	70634.00 ± 58.91	
solution	0.1016 ± 0.0015	0.1141 ± 0.0036	5.63 ± 0.69	RA, DEC, F[0], F[1], Δt
PRM-B6	0.0000 ± 0.0859	0.0000 ± 0.0859	70634.00 ± 58.91	
solution	0.0791 ± 0.0004	0.2948 ± 0.0028	2.68 ± 0.68	RA, DEC, F[0], F[1], Δt
PRM-B7	0.0000 ± 0.0859	0.0000 ± 0.0859	70634.00 ± 58.91	
solution	0.0398 ± 0.0015	0.1603 ± 0.0092	-24.43 ± 0.74	RA, DEC, F[0], F[1], Δt
TSM-B1	0.0000 ± 0.0859	0.0000 ± 0.0859	17495.00 ± 14.76	
solution	0.0104 ± 0.0008	0.0904 ± 0.0006	1.33 ± 0.51	F[0], F[1], RA, DEC, Δt
TSM-B2	0.0000 ± 0.0859	0.0000 ± 0.0859	2065.00 ± 2.90	
solution	0.0855 ± 0.0074	0.4212 ± 0.0026	-6.27 ± 0.21	F[0], F[1], RA, DEC, Δt

Table 2: Maneuver execution errors for the GRAIL-B spacecraft. Total pointing error is less than RA error in some cases as RA and declination are correlated. *LOI-B lists F_0 in Newtons for the thrust model instead of ΔV as the ΔV conversion was not available for LOI.

Tables 4 through 11 the results for fitting all maneuvers.

4.1 TLC A

The first GRAIL-A trajectory correction maneuver, TCM-A1, was canceled. Reconstruction of the first trajectory correction maneuver, TCM-A2, gives value within 2σ for pointing and 1σ for ΔV as shown in Figure 2. TCM-A2 maneuver had RA error of -0.2761 ± 0.0008 degrees, declination error of -0.0476 ± 0.0033 degrees, and ΔV error of 0.34 ± 0.59 mm/s. No improvement in the final uncertainties was seen over the original orbit determination (OD) solution delivered during operations, which will be referred to in this report as the 'OD solution'. The maneuver executed within 2 σ for RA, 1 σ for declination, and 0.1 σ for ΔV. The reconstructed solution agrees with the original solution within 1 σ for pointing and ΔV. A data arc sensitivity analysis of the TCM-A2 maneuver was performed. This analysis showed the estimate is sensitive to the data arc length particularly for 1 day versus 1 week data arc lengths as shown in Table 3. TCM-A1 was designed but was canceled.

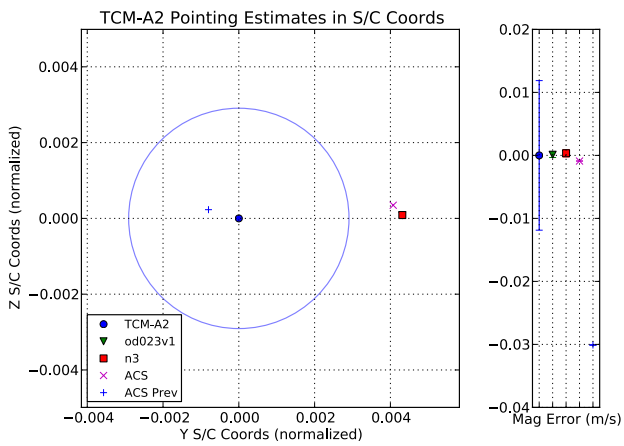

Figure 2: TCM-A2 reconstruction. 'n3' refers to the reconstructed solution using the designed polynomial main engine force model. Parameters estimated in 'n3' are RA, declination, and

Maneuver	**RA (degrees)**	**Dec. (degrees)**	F_0 **(N)**
TCM-A2	119.0000 ± 0.09560	-2.5600 ± 0.09550	26.9000 ± 0.0224
Solution	**RA error**	**Dec. error**	F_0 **error**
1 day	-0.2020 ± 0.08450	-0.0414 ± 0.0082	0.1910 ± 0.0215
1 week	-0.2760 ± 0.0008	-0.0460 ± 0.0045	0.189 ± 0.0210
2 weeks	-0.2770 ± 0.0006	-0.0466 ± 0.0024	0.191 ± 0.0209
3 weeks	-0.2760 ± 0.0006	-0.0466 ± 0.0024	0.185 ± 0.0021
4 weeks	-0.2760 ± 0.0006	-0.0466 ± 0.0024	0.185 ± 0.0021

Table 3: Sensitivity of TCM-A2 fit to DCO cut off time and comparison to original solution. Solution name indicates duration of data included after TCM-A2 maneuver.

The TCM-A3 maneuver had RA error of -0.0246 ± 0.0016 degrees, declination error of -0.0654 ± 0.0077 degrees, and ΔV error of -2.62 ± 0.52 mm/s. A $\sim 10\%$ improvement in uncertainties was seen in the reconstructed solution compared to the OD solution. The maneuver executed within 0.5 σ for RA, 1 σ for declination, and 0.5 σ for ΔV. The reconstructed solution agrees with the original solution within 1σ for pointing and ΔV.

As shown in Table 4 and Figure 3, the TCM-A4 maneuver had RA error of 0.0305 ± 0.0706 degrees, declination error of 0.1287 ± 0.00933 degrees, and ΔV error of -5.32 ± 0.37 mm/s as shown in Table 4. No improvement in uncertainties was seen in the reconstructed solution compared to the OD solution. The maneuver executed within 0.5 σ for RA, 1 σ for declination, and 4 σ for ΔV. The reconstructed solution agrees with the original solution within 3 σ for RA, 5 σ for declination, and 1 σ for ΔV. Issues arose with the analysis due to the burn being 20% longer than designed (17.8 s vs. 14.8 s). This caused for the polynomial describing the designed burn force to be inaccurate for the longer duration. This issue was avoided by modeling and estimating a constant thrust and mass flow rate for the burn.

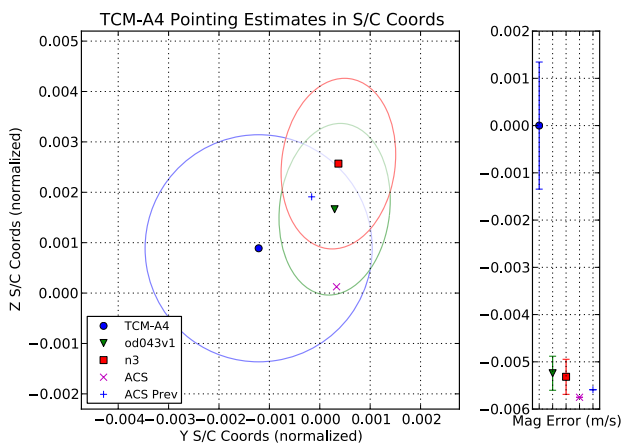

Figure 3: TCM-A4 reconstruction. 'n3' refers to the reconstructed solution using a linear main engine force model. The circle around a maneuver fit represents the execution model 1 σ [2]. Normalized coordinates are approximately radians for small angles.

Maneuver	Y (deg)	Z (deg)	ΔV (mm/s)	Est. parameters
TCM-A4	0.0000 ± 0.1318	0.0000 ± 0.0509	234.00 ± 1.34	
Solution				
Epoch	**Y error**	**Z error**	**ΔV error**	
DCO				
od043v1				
16-NOV-2011 18:30 UTC	0.0864 ± 0.0630	0.0444 ± 0.0974	-5.24 ± 0.36	ΔV, RA, DEC, t_0
20-DEC-2011 08:00 UTC				
n3				
16-NOV-2011 20:00 UTC	0.0907 ± 0.0630	0.0963 ± 0.0974	-5.32 ± 0.37	RA, DEC, F[0], Δt
31-DEC-2011 00:00 UTC				

Table 4: TCM-A4 reconstruction compared with the delivered OD during operations. 'n3' refers to the reconstructed solution using a linear main engine force model.

4.2 TLC B

The execution analysis for the TLC maneuvers were in close agreement between the original and reconstructed solutions for the TLC B maneuvers. No reductions in uncertainty were reached.

The first GRAIL-B designed trajectory correction maneuver, TCM-B1, was canceled. As shown in Table 5 and Figure 4, the first trajectory correction maneuver for GRAIL-B, TCM-B2, maneuver

had RA error of 0.0674 ± 0.0010 degrees, declination error of -0.3001 ± 0.0011 degrees, and ΔV error of -8.60 ± 1.41 mm/s as shown in Table 5. No improvement in uncertainties was seen in the reconstructed solution compared to the OD solution. The maneuver executed within 0.5 σ for RA, 2 σ for declination, and 0.5 σ for ΔV. The reconstructed solution agrees with the original solution within 1 σ for RA, 1 σ for declination, and 3 σ for ΔV. The TCM-B2 maneuver likely featured an out-gassing event during the slew just before the maneuver. During a maneuver, the satellite slews to align the main engine with the thrust direction. This may have exposed portions of the spacecraft to the Sun for the first time, which can create significant out-gassing events.

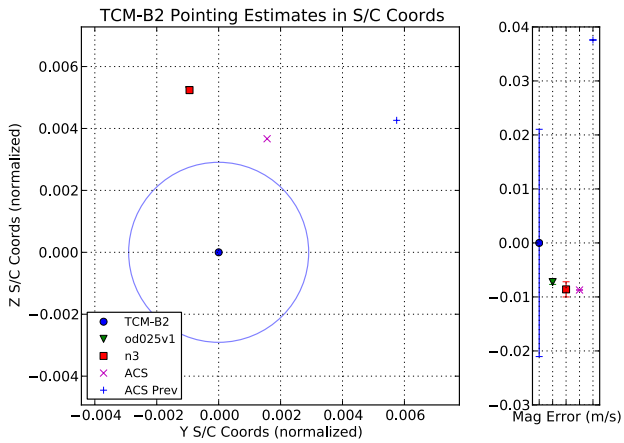

Figure 4: TCM-B2 reconstruction. 'n3' refers to the reconstructed solution using the polynomial main engine force model. The OD solution and the reconstruction solution nearly overlap in pointing.

Maneuver	Y (deg)	Z (deg)	ΔV (mm/s)	Est. parameters
TCM-B2	0.0000 ± 0.1662	0.0000 ± 0.0000	25096.00 ± 21.04	
Solution				
Epoch	**Y error**	**Z error**	**ΔV error**	
DCO				
od025v1				
23-SEP-2011 01:00 UTC	-0.0545 ± 0.0005	0.3001 ± 0.0011	-7.23 ± 0.45	RA, DEC, F[0], F[1]
13-NOV-2011 21:35 UTC				
n3				
11-SEP-2011 20:00 UTC	-0.0539 ± 0.0007	0.3002 ± 0.0011	-8.60 ± 1.41	RA, DEC, F[0], Δt
24-OCT-2011 12:00 UTC				

Table 5: TCM-B2 reconstruction compared with the delivered OD during operations. 'n3' refers to the reconstructed solution using the polynomial main engine force model.

The TCM-B3 maneuver had RA error of -0.2276 ± 0.0014 degrees, declination error of -0.1350 ± 0.0044 degrees, and ΔV error of -2.54 ± 0.48 mm/s. A $\sim$15 % improvement in pointing and $\sim$6 % improvement in ΔV uncertainties was calculated for the reconstructed solution compared to the OD solution. The maneuver executed within 2 σ for RA, 1 σ for declination, and 0.5 σ for ΔV. The reconstructed solution agrees with the original solution within 1 σ for RA, 1 σ for declination, and 1 σ for ΔV. The TCM-B4 maneuver had RA error of -0.0280 ± 0.0067 degrees, declination error of 0.0110 ± 0.0660 degrees, and ΔV error of -0.19 ± 0.36 mm/s. No improvement in uncertainties

were calculated compared to the OD solution. The maneuver executed within 0.3 σ for RA, 0.1 σ for declination, and 0.2 σ for ΔV. Reconstructed values agree with the original solution within 1 σ for RA, declination, and ΔV.

4.3 LOI-A

As shown in Table 6, the LOI-A maneuver had RA error of -0.0044 ± 0.0082 degrees (which is measured with respect to the spacecraft frame rotating at a constant pitch rate), declination error of -0.0643 ± 0.0063 degrees (which is with respect to the spacecraft frame), and F_0 error of 0.6034 ± 0.0008 N. The RA uncertainty is an order of magnitude lower than the original solution. Uncertainties were calculated compared to the OD solution. The maneuver executed within 0.03σ for RA, 1 σ for declination, and 1 σ for F_0. Reconstructed values agree with the original solution within 3 σ for RA, 15 σ for declination, and 1 σ for F_0.

Maneuver	**RA (deg)**	**DEC (deg)**	**F[0] (N)**	**Est. parameters**
LOI-A	0.0000 ± 0.2300	0.0000 ± 0.0830	33.5089 ± 0.6560	
Solution				
Epoch	**RA error**	**DEC error**	**F[0] error**	
DCO				
od051v5				
30-DEC-2011 11:50 UTC	-0.0270 ± 0.0920	-0.1830 ± 0.0085	0.6485 ± 0.3547	ΔV, RA, DEC, F[0], F[1], t_0
01-Jan-2012 04:00 UTC				
n3				
09-DEC-2011 20:00 UTC	-0.3730 ± 0.0110	-0.4000 ± 0.0120	0.6034 ± 0.0008	RA, DEC, F[0], Δt
01-JAN-2012 00:00 UTC				

Table 6: LOI-A reconstruction compared with the delivered OD during operations. 'n3' refers to the reconstructed solution using the designed polynomial main engine force model. RA and declination are measured with respect to the spacecraft frame

4.4 LOI-B

As shown in Table 7, the LOI-B maneuver had RA error of -0.2199 ± 0.0064 degrees (which is measured with respect to the spacecraft frame rotating at a constant pitch rate), declination error of -0.1684 ± 0.0011 degrees (which is also measured with respect to the spacecraft frame), and F_0 error of 0.2510 ± 0.0008 N as shown in Table 7. The RA uncertainty is an order of magnitude lower than the OD solution and the declination uncertainty is also an order of magnitude smaller than the OD solution. The maneuver executed within 1σ for RA, 2σ for declination, and 1.5 σ for F_0. Reconstructed values agree with the original solution within 2.5 σ for RA, 2 σ for declination, and 4 σ for F_0.

Maneuver	RA (deg)	DEC (deg)	F[0] (N)	Est. parameters
LOI-B	0.0000 ± 0.2300	0.0000 ± 0.0830	34.1695 ± 0.2187	
Solution				
Epoch	**RA error**	**DEC error**	**F[0] error**	
DCO				
od053v4				
01-JAN-2012 16:00 UTC	-0.0270 ± 0.0920	-0.1830 ± 0.0085	0.0036 ± 0.0643	ΔV, RA, DEC, F[0], F[1], t_0
02-JAN-2012 00:00 UTC				
n3				
14-DEC-2011 20:00 UTC	-0.3730 ± 0.0110	-0.4000 ± 0.0120	0.2510 ± 0.0008	RA, DEC, F[0], Δt
02-JAN-2012 04:10 UTC				

Table 7: LOI-B reconstruction compared with the delivered OD during operations. 'n3' refers to the reconstructed solution using the designed polynomial main engine force model. RA and declination are measured with respect to the spacecraft frame

4.5 OPR A

Each OPR-A maneuver was modeled using the 6th-order polynomial thruster model and a linear thruster force model estimated from telemetry. Typical data arcs included data 2.5 revolutions before a maneuver and 0.5 revolutions after a maneuver. Pointing error was below 0.5 degrees. Typical ΔV error for all maneuvers, with ΔV $\sim$ 75 m/s, was below 30 mm/s with uncertainty $\sim$1.0 mm/s.

The PRM-A1 reconstructions have similar uncertainty to the original solution and ΔV error about 80% of the OD solution. The maneuver executed within 0.5σ for RA, 2.5σ for declination, and 0.5 σ for ΔV. Reconstructed polynomial thrust model values agree with the original solution within 10 σ for RA, 25 σ for declination, and 3 σ for ΔV. The PRM-A2 maneuver executed within 0.5 σ for RA, 2 σ for declination, and 0.5 σ for ΔV. The polynomial thrust model reconstruction gave RA, Dec., and ΔV uncertainty that is 25% of the original solution. Reconstructed values agree with the original solution within 6 σ for RA, 3 σ for declination, and 4 σ for ΔV. The PRM-A3 maneuver executed within 1 σ for RA, 2 σ for declination, and 0.5 σ for ΔV. The polynomial thrust model reconstruction gave RA, declination , and ΔV uncertainty that is 80% of the original solution. Reconstructed polynomial thrust model values agree with the original solution within 2 σ for RA, 2 σ for declination, and 1 σ for ΔV.

As shown in Table 8 and Figure 5, the PRM-A4 maneuver executed within 0.5 σ for RA, 1 σ for declination, and 0.2 σ for ΔV. The polynomial thrust model reconstruction gave RA, declination, and ΔV uncertainties that are 25% of the original solution. Reconstructed polynomial thrust model values agree with the original solution within 3.5 σ for RA, 4 σ for declination, and 1 σ for ΔV.

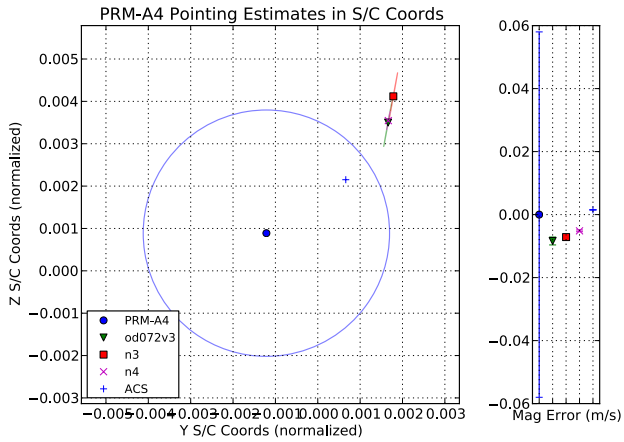

Figure 5: PRM-A4 reconstruction. 'n3' refers to the reconstructed solution using the polynomial main engine force model and 'n4' refers to the reconstructed solution using the linear main engine force model. The 'n4' solution and the OD solution nearly overlap in pointing.

Maneuver	**Y (deg)**	**Z (deg)**	**ΔV (mm/s)**	**Est. parameters**
PRM-A4	0.0000 ± 0.1662	0.0000 ± 0.0509	69544.00 ± 58.00	
Solution				
Epoch	**Y error**	**Z error**	**ΔV error**	
DCO				
od072v3				
24-JAN-2012 11:45 UTC	0.1646 ± 0.0057	0.1497 ± 0.0321	-8.38 ± 1.25	RA, DEC, F[0], F[1], Δt
24-JAN-2012 16:40 UTC				
n3				
24-JAN-2012 02:30 UTC	0.1717 ± 0.0057	0.1851 ± 0.0315	-7.13 ± 0.34	RA, DEC, F[0], F[1], Δt
24-JAN-2012 17:20 ET				
n4				
24-JAN-2012 02:30 UTC	0.1649 ± 0.0022	0.1522 ± 0.0120	-5.16 ± 0.28	RA, DEC, F[0], F[1], Δt
24-JAN-2012 17:20 ET				

Table 8: PRM-A4 reconstruction compared with the delivered OD during operations. 'n3' refers to the reconstructed solution using the polynomial main engine force model and 'n4' refers to the reconstructed solution using the linear main engine force model.

The PRM-A5 maneuver executed within 0.1 σ for RA, 1.5 σ for declination, and 0.2 σ for ΔV. The polynomial thrust model reconstruction gave RA, declination, and ΔV uncertainties that are 10% of the original solution's uncertainties. Reconstructed polynomial thrust model values agree with the original solution within 2 σ for RA, 2 σ for declination, and 1 σ for ΔV. The PRM-A6 maneuver executed within 1 σ for RA, 1.5 σ for declination, and 0.4 σ for ΔV. The linear thrust model reconstruction gave RA, declination, and ΔV uncertainties that are similar to the original solution's uncertainties. Reconstructed linear thrust model values agree with the original solution within 2 σ for RA, 2 σ for declination, and 4 σ for ΔV. The PRM-A7 maneuver executed within 0.5 σ for RA, 1.7 σ for declination, and 0.4 σ for ΔV. The linear thrust model reconstruction gave RA, declination, and ΔV uncertainties that are similar to the original solution's uncertainties. Reconstructed linear thrust model values agree with the original solution within 10 σ for RA, 10 σ

for declination, and 6 σ for ΔV.

4.6 OPR B

Each OPR-B maneuver was also modeled using the 6th-order designed thruster model and a linear thruster force model estimated from telemetry. Typical data arcs included data 2.5 revolutions before a maneuver and 0.5 revolutions after a maneuver. Typical pointing error was below 0.3 degrees. Typical ΔV error for all maneuvers, with ΔV $\sim$ 70 m/s, was below 25 mm/s with uncertainty $\sim$0.8 mm/s.

As shown in Table 9 and Figure 6, the PRM-B1 maneuver executed within 0.5 σ for RA, 1.5 σ for declination, and 0.3 σ for ΔV. The polynomial thrust model reconstruction gave RA, declination, and ΔV uncertainties that are similar to the original solution's uncertainties for pointing and ΔV uncertainty 30% of the original solution. Reconstructed polynomial thrust model values agree with the original solution within 15 σ for RA, 4 σ for declination, and 1 σ for ΔV.

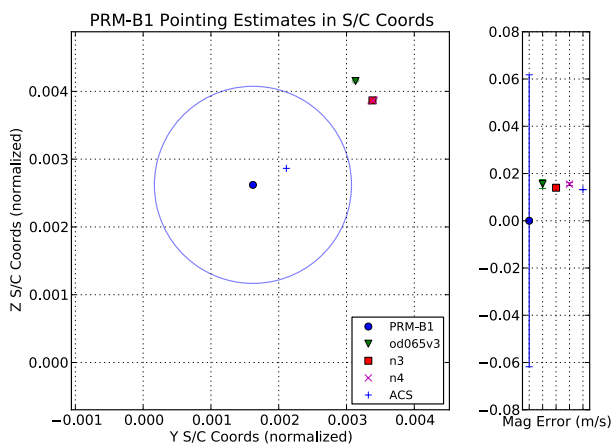

Figure 6: PRM-B1 reconstruction. 'n3' refers to the reconstructed solution using the polynomial main engine force model with estimation of a constant and linear force term. 'n4' refers to the reconstructed solution using the linear main engine force model. 'n3' and 'n4' pointing solutions essentially overlap. 'n5', which is a polynomial force model, constant force term estimate solution shown in Table 9, shows up in the third quadrant.

Maneuver	Y (deg)	Z (deg)	ΔV (mm/s)	Est. parameters
PRM-B1	0.0000 ± 0.0859	0.0000 ± 0.1502	74109.00 ± 61.80	
Solution				
Epoch	**Y error**	**Z error**	**ΔV error**	
DCO				
od065v3				
13-JAN-2012 14:30 UTC	0.0867 ± 0.0029	0.0878 ± 0.0017	15.56 ± 1.88	RA, DEC, F[0], F[1], Δt
13-JAN-2012 23:45 UTC				
n3				
12-JAN-2012 04:44 UTC	0.1010 ± 0.0038	0.0714 ± 0.0031	13.98 ± 0.61	RA, DEC, F[0], F[1], Δt
13-JAN-2012 23:00 UTC				
n4				
12-JAN-2012 04:44 UTC	0.1015 ± 0.0038	0.0713 ± 0.0031	15.51 ± 0.62	RA, DEC, F[0], F[1], Δt
13-JAN-2012 23:00 UTC				
n5				
12-JAN-2012 04:44 UTC	-0.0990 ± 0.0103	-0.0905 ± 0.0120	19.18 ± 0.42	RA, DEC, F[0], Δt
13-JAN-2012 23:00 UTC				

Table 9: PRM-B1 reconstruction compared with the delivered OD during operations. 'n3' refers to the reconstructed solution using the polynomial main engine force model and 'n4' refers to the reconstructed solution using the linear main engine force model. 'n5' refers to the reconstructed solution using the polynomial main engine force model with estimation of a constant force term only.

The accelerations of GRAIL-B from the linear and polynomial thrust models used in the reconstructions is shown in Figure 7 plotted against the spacecraft X acceleration from accelerometer telemetry data from the actual burn.

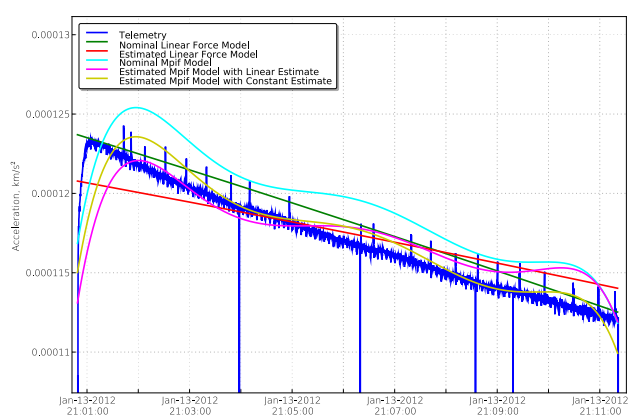

Figure 7: Nominal and estimated linear thrust model estimated from telemetry and nominal and estimated designed polynomial thrust model plotted against the acceleromter telemetry from the TCM-B1 maneuver.

The PRM-B2 maneuver executed within 0.5 σ for RA, 1 σ for declination, and 0.1 σ for ΔV. The polynomial thrust model reconstruction gave RA, declination, and ΔV uncertainties that are similar to the original solution's uncertainties for pointing and 60% smaller for ΔV uncertainty. Reconstructed polynomial thrust model values agree with the original solution within 1 σ for RA, 1

σ for declination, and 1 σ for ΔV. The PRM-B3 maneuver executed within 0.7 σ for RA, 0.3 σ for declination, and 0.1 σ for ΔV. The polynomial thrust model reconstruction gave RA, declination, and ΔV uncertainties that are similar to the original solution's uncertainties for pointing and 70% smaller for ΔV uncertainty. Reconstructed polynomial thrust model values agree with the original solution within 1 σ for RA, 1 σ for declination, and 2 σ for ΔV. The PRM-B4 maneuver executed within 1.5 σ for RA, 1.0 σ for declination, and 0.4 σ for ΔV. The polynomial thrust model reconstruction gave RA, declination, and ΔV uncertainties that are similar to the original solution's uncertainties for pointing and ΔV uncertainty. Reconstructed polynomial thrust model values agree with the original solution within 20 σ for RA, 1 σ for declination, and 20 σ for ΔV.

The PRM-B5 maneuver executed within 2.0 σ for RA, 1.0 σ for declination, and 0.1 σ for ΔV. The polynomial thrust model reconstruction gave RA, declination, and ΔV uncertainties that are similar to the original solution's uncertainties for pointing and 400% for ΔV. Reconstructed polynomial thrust model values agree with the original solution within 5 σ for RA, 10 σ for declination, and 10 σ for ΔV. The PRM-B6 maneuver executed within 4.0 σ for RA, 0.4 σ for declination, and 0.1σ for ΔV. The polynomial thrust model reconstruction gave RA, declination and ΔV uncertainties that are similar to the original solution's uncertainties for pointing and 40% for ΔV. Reconstructed polynomial thrust model values agree with the original solution within 10 σ for RA, 40 σ for declination, and 0.5 σ for ΔV. The PRM-B7 maneuver executed within 2 σ for RA, 0.2 σ for declination, and 0.5σ for ΔV. The polynomial thrust model reconstruction gave RA, declination, and ΔV uncertainties that are similar to the original solution's uncertainties for pointing and ΔV. Reconstructed polynomial thrust model values agree with the original solution within 50 σ for RA, 1 σ for declination, and 45 σ for ΔV.

4.7 TSF A

Each TSF-A maneuver was also modeled using the 6th-order designed thruster model and a linear thruster force model estimated from telemetry. TSM-A1 executed with ΔV error of 4.0 mm/s and pointing error of 0.45 degrees. TSM-A2 executed with ΔV error of 2.5 mm/s and pointing error of 0.06 degrees. Typical data arcs included data 1.5 revolutions before a maneuver and 1.5 revolutions after a maneuver.

The TSM-A1 maneuver executed within 5 σ for RA, 3.5 σ for declination, and 0.6 σ for ΔV. The polynomial thrust model reconstruction gave RA, declination, and ΔV uncertainties that are similar to the original solution's uncertainties for pointing and ΔV that are $\sim$ 50% of the original solution. Reconstructed polynomial thrust model values agree with the original solution within 4 σ for RA, 20 σ for declination, and 1 σ for ΔV. The TSM-A2 maneuver executed within 0.7 σ for RA, 0.1 σ for declination, and 0.3σ for ΔV. The polynomial thrust model reconstruction gave RA and declination uncertainties that are $\sim$ 70% of the original solution and uncertainties in ΔV that are 25% of the original solution. Reconstructed polynomial thrust model values agree with the original solution within 1 σ for RA, 2 σ for declination, and 1 σ for ΔV.

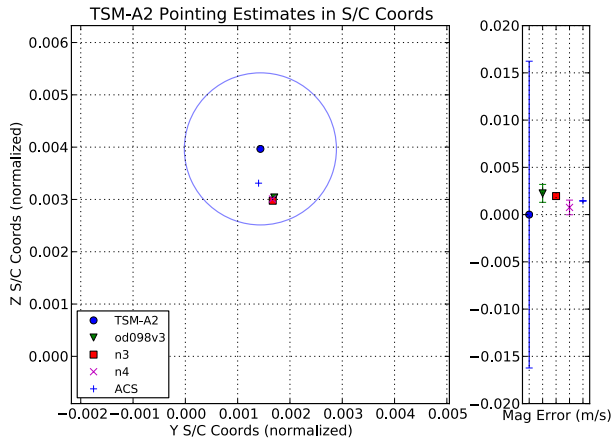

Figure 8: TSM-A2 reconstruction. 'n3' refers to the reconstructed solution using the polynomial main engine force model and 'n4' refers to the reconstructed solution using the linear main engine force model.

Maneuver	Y (deg)	Z (deg)	ΔV (mm/s)	Est. parameters
TSM-A2	0.0000 ± 0.0859	0.0000 ± 0.2273	19276.00 ± 16.23	
Solution				
Epoch	**Y error**	**Z error**	**ΔV error**	
DCO				
od098v3				
20-FEB-2012 13:07 UTC	0.0152 ± 0.0010	-0.0532 ± 0.0021	2.25 ± 0.95	RA, DEC, F[0], Δt
20-FEB-2012 18:00 UTC				
n3				
20-FEB-2012 09:48 UTC	0.0135 ± 0.0003	-0.0568 ± 0.0014	1.96 ± 0.21	RA, DEC, F[0], F[1], Δt
20-FEB-2012 17:22 UTC				
n4				
20-FEB-2012 09:48 UTC	0.0132 ± 0.0007	-0.0550 ± 0.0014	0.76 ± 0.77	RA, DEC, F[0], F[1], Δt
20-FEB-2012 17:22 UTC				

Table 10: TSM-A2 reconstruction compared with the delivered OD during operations.

4.8 TSF B

Each TSF-B maneuver also was modeled using the 6th-order designed thruster model and a linear thruster force model estimated from telemetry. TSM-B1 executed with ΔV error of 1.5 mm/s and pointing error of 0.10 degrees. TSM-B2 executed with ΔV error of -6.3 mm/s and pointing error of 0.43 degrees. Typical data arcs included data 1.5 revolutions before a maneuver and 1.5 revolutions after a maneuver.

The TSM-B1 maneuver executed within 0.5 σ for RA, 1 σ for declination, and 0.1σ for ΔV. The polynomial thrust model reconstruction gave pointing uncertainties that are $\sim$ 50% of the original solution and ΔV uncertainties that are similar to the original solution. Reconstructed polynomial thrust model values agree with the original solution within 5 σ for RA, 6 σ for declination, and 6 σ for ΔV. As shown in Table 11 and Figure 9, the TSM-B2 maneuver executed with large error

with 5 σ for RA, 0.2 σ for declination, and 3σ for ΔV. The polynomial thrust model reconstruction gave RA, declination, and ΔV uncertainties that are $\sim$ 20% of the original solution. Reconstructed polynomial thrust model values agree with the original solution within 1 σ for RA, 0.1 σ for declination, and 1.5 σ for ΔV.

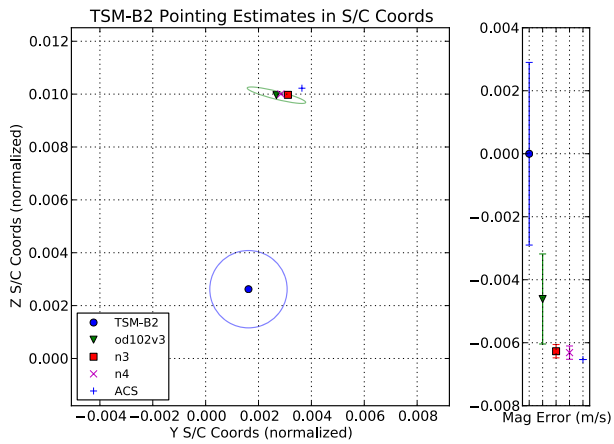

Figure 9: TSM-B2 reconstruction. 'n3' refers to the reconstructed solution using the polynomial main engine force model and 'n4' refers to the reconstructed solution using the linear main engine force model. The linear force model solution and the OD solution nearly overlap in pointing.

Maneuver	Y (deg)	Z (deg)	ΔV (mm/s)	Est. parameters
TSM-B2	0.0000 ± 0.0859	0.0000 ± 0.1502	2065.00 ± 2.90	
Solution				
Epoch	**Y error**	**Z error**	**ΔV error**	
DCO				
od102v3				
24-FEB-2012 13:40 UTC	0.0606 ± 0.0630	0.4204 ± 0.0178	-4.61 ± 1.43	F[0], RA, DEC, Δt
24-FEB-2012 20:20 UTC				
n3				
24-FEB-2012 13:40 UTC	0.0855 ± 0.0074	0.4212 ± 0.0026	-6.27 ± 0.21	F[0], F[1], RA, DEC, Δt
24-FEB-2012 20:00 UTC				
n4				
24-FEB-2012 13:40 UTC	0.0704 ± 0.0074	0.4232 ± 0.0026	-6.31 ± 0.21	F[0], F[1], RA, DEC, Δt
24-FEB-2012 20:00 UTC				

Table 11: TSM-B2 reconstruction compared with the delivered OD during operations. 'n3' refers to the reconstructed solution using the polynomial main engine force model and 'n4' refers to the reconstructed solution using the linear main engine force model.

5 Analysis

Pointing error was consistently in the positive Y and Z directions relative to the designed maneuver during OPR for both spacecraft. TLC-A maneuvers also are grouped in this area while TLC-B maneuver executed more randomly. TSF-A and TSF-B maneuvers executed more randomly. Most of the TLC maneuvers executed with a smaller ΔV than designed. All the OPR-A maneuvers have

smaller ΔV than designed. OPR-B ΔV errors were fairly random. An alternate linear force model with a linear estimate was attempted for OPR maneuvers along with the polynomial force model. The alternate linear force model analysis strategy, which included a linear force model calculated from maneuver telemetry acceleration data and estimation of the constant and linear force terms, used in modeling OPR and TSF data gave similar pointing error to the baseline strategy, which included the delivered maneuver polynomial force model used in operations and estimation of the constant and linear force terms. If time permits, a strategy using a two function force model or a linear force model with a constant estimation will be investigated.

6 Conclusion

For TLC-A, all maneuvers executed with ΔV errors below -5.50 $\pm$0.50 mm/s and pointing errors below 0.25 degrees. For LOI, OPR, and TSF maneuvers, GRAIL-A executed maneuvers with ΔV errors below 30.0 mm/s and pointing error below 0.51 degrees. Pointing errors were generally found to have executed within 2 σ for pointing and 1 σ for ΔV for all maneuvers. For LOI, OPR, and TSF maneuvers, GRAIL-A executed maneuvers with ΔV errors below 30.0 mm/s and pointing error below 0.51 degrees. For TLC-B, all maneuvers executed within ΔV error of -8.60 mm/s $\pm$1.41 mm/s and pointing error of 0.300 degrees. GRAIL-B maneuvers in lunar orbit executed with maximum ΔV errors of 25.0 mm/s and pointing error of 0.43 degrees. Finally, RA and declination were found to be sensitive to data arc length. Several studies were done to compare different orbit determination strategies. Maneuver pointing was found to be sensitive to data arc length. An alternative strategy using a linear force model estimated from telemetry gave similar execution error and uncertainty to the baseline strategy using the polynomial force model delivered during operations. A linear force model was found to fit the data better than the nominal designed 6th order polynomial. OPR-A and OPR-B maneuvers were consistently biased towards the first quadrant in the spacecraft Y-Z plane. These maneuver reconstructions will enable the GRAIL Navigation Team to better characterize the main engine performance of each spacecraft. This work was done to help improve the dynamic models used for orbit determination. This should help the Navigation Team to navigate low ($>$ 8 km) altitude orbits during the extended-mission phase in the fall of 2012.

7 Acknowledgments

This research was carried out at the Jet Propulsion Laboratory, California Institute of Technology, and was sponsored by the NASA Space Grant Program and the National Aeronautics and Space Administration.

References

[1] P. Antreasian et al. *Gravity Recovery and Interior Laboratory (GRAIL) Project: Navigation Plan.* Jet Propulsion Laboratory, 2010.

[2] T. Goodson. Grail maneuver execution-error tracking, 2012.

[3] T. Wang, J.B. Collier, J.E. Ekelund, and P.J Breckheimer. Applications of square-root information filtering and smoothing in spacecraft orbit determination. *Proceedings of the 27th IEEE Conference on Decision and Control*, 1988.